Supplementary Information

A photoelectrochemical cytosensor based on Bi_2S_3-MoS_2 heterojunction-modified reduced oxide graphene honeycombs film for sensitive detection of circulating tumor cells

Yuhong Guo,[a ‡] Binbin Guo,[a ‡] Zhaopeng Liu,[a] Jian Li,[a] Liming Gao,[b,*] Hong, Jiang,[a,*] Jidong Wang[a,*]

a State Key Laboratory of Metastable Materials Science and Technology, Nano-biotechnology Key Lab of Hebei Province, Yanshan University, Qinhuangdao 066004, China

b The First Hospital in Qinhuangdao, Qinhuangdao, 066004, China

‡ These authors contributed equally

***Corresponding author.**
Jidong Wang
Email address: wangjidong@ysu.edu.cn

Tel.: +86-335-807-4648; **Fax:** +86-335-807-4648;
Address: College of Environmental and Chemical Engineering, Yanshan University, Qinhuangdao 066004, China

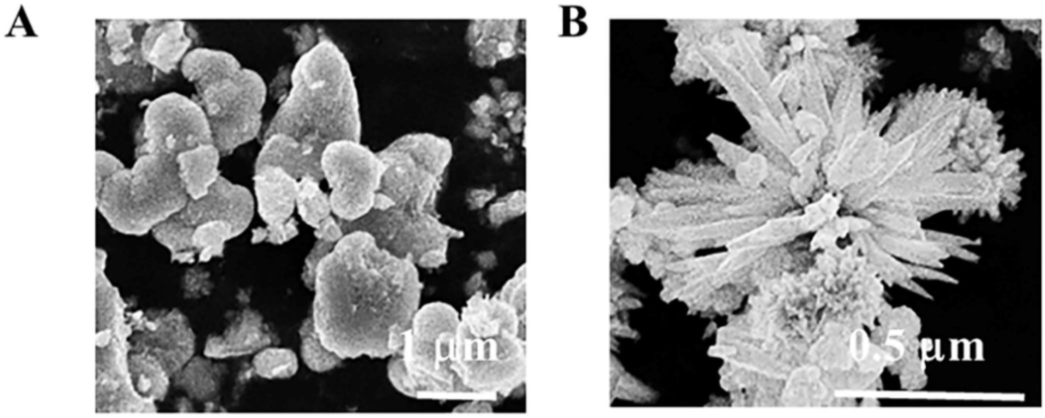

Fig. S1. SEM images of MoS_2 nanosheets(Fig. S1A) and Bi_2S_3 micro-flowers structure (Fig. S1B).

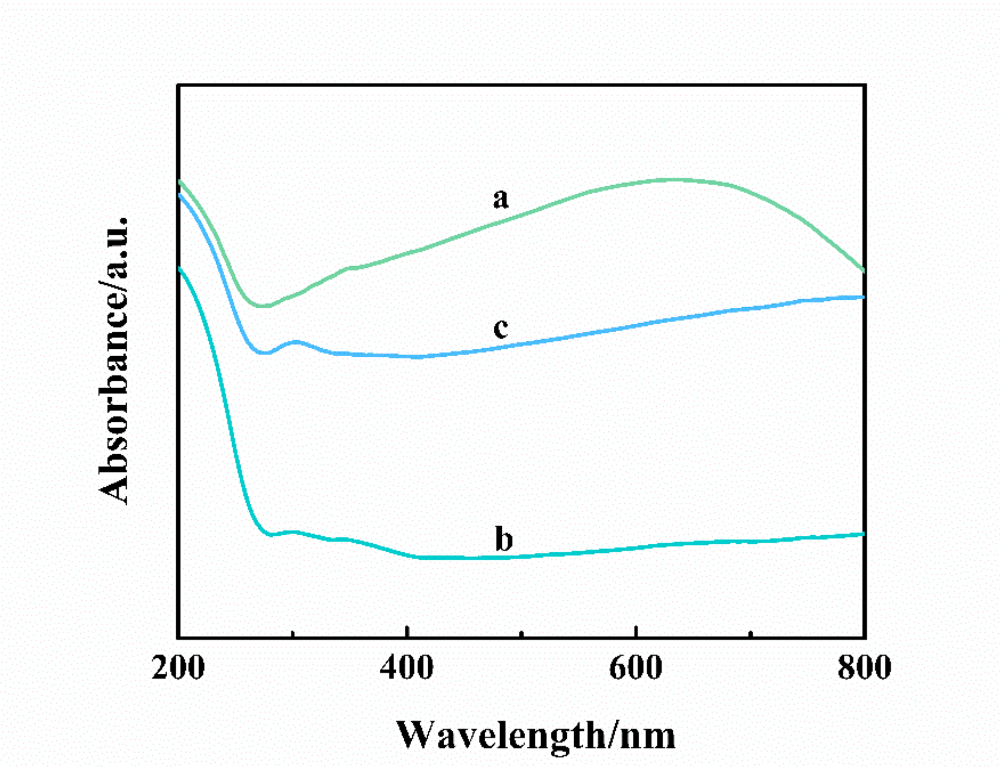

Fig. S2. The UV–Vis absorption spectra of Bi_2S_3 (a), MoS_2 (b) and MoS_2-Bi_2S_3 heterojunction(c).

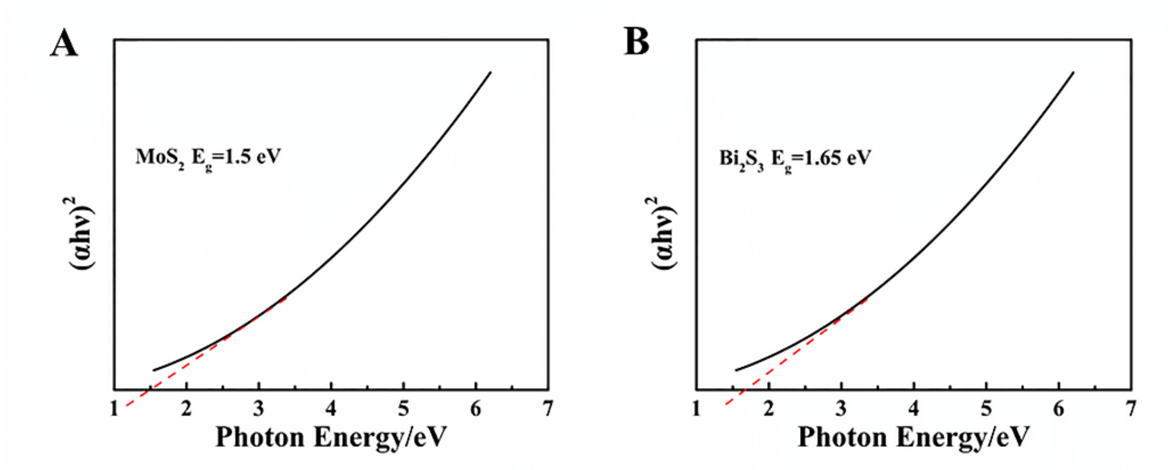

Fig.S3. The Tauc plots for the band gap energy of MoS_2 and Bi_2S_3

For an inorganic semiconductor, the optical band gaps can be calculated according to the Tauc approach by using the following equation[2]: $\alpha hv = A(hv\text{-}Eg)^{n/2}$ Where α, h, v, A, Eg represent the absorption coefficient, Planck constant, light frequency, a constant and the band gap energy, respectively. The band gap can be estimated from the intercept of the tangent to the plot. As shown in Figure S3, the band gap of MoS_2, $Bi_2S_3$and are 1.5 eV, 1.65 eV respectively.

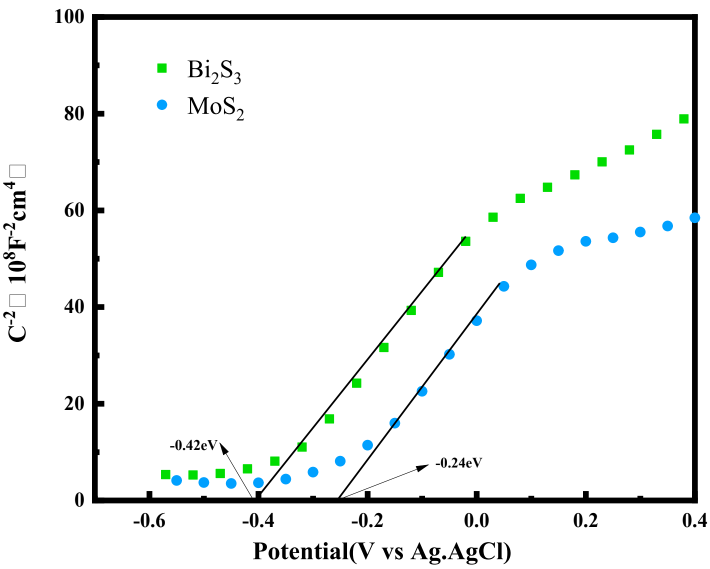

Fig. S4 Mott-Schottky curves of the MoS_2 and Bi_2S_3.

The electrode potential versus Ag/AgCl electrode are converting to the NHE potential using this equation[1]: $E_{fb(vs.NHE)} = E_{fb(vs.Ag/Agcl)} + 0.197$

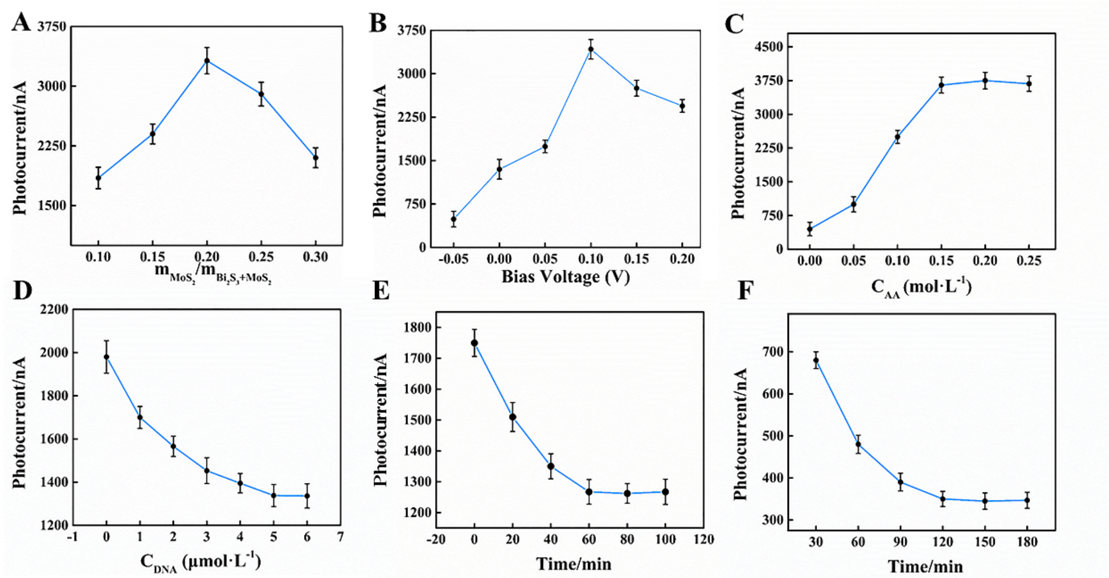

Fig. S5 (A) Photocurrent plots for different MoS_2 mass fractions; (B) Photocurrent plots at different bias voltage; (C) Photocurrent responses for different AA concentrations; (D) Photocurrent responses different DNA concentration (E) Photocurrent responses of different DNA incubation time; (F) Photocurrent responses of different cell incubation time.

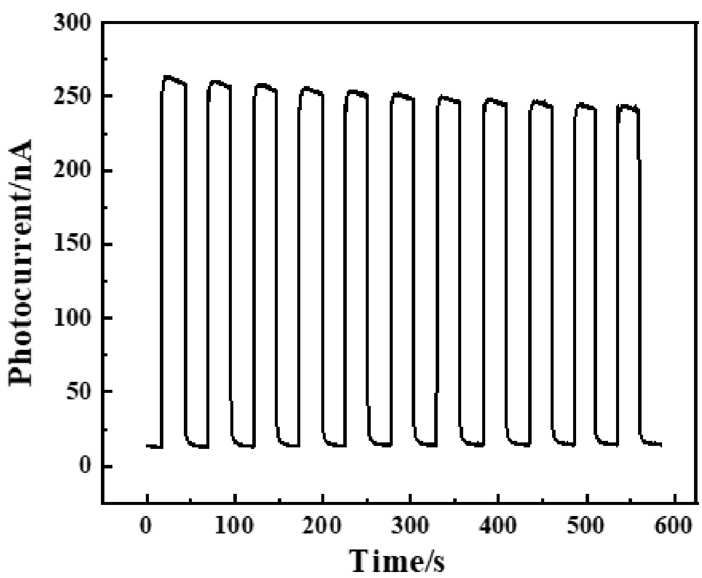

Fig. S6 Photocurrent response of the sensor under continuous excitation

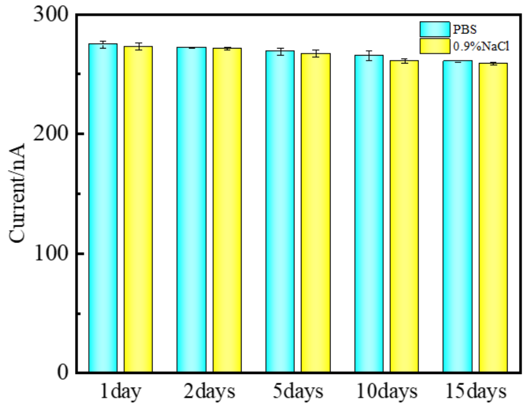

Fig. S7 Photocurrent response of the sensor in various buffers

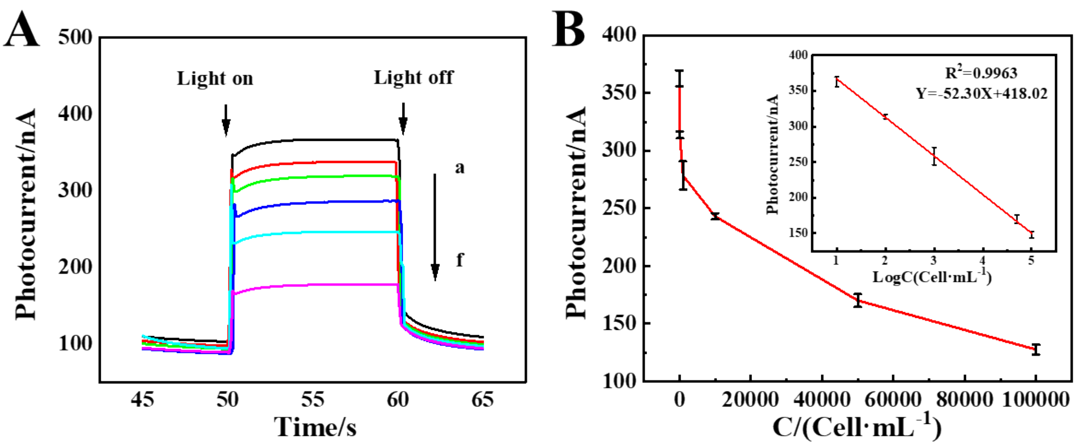

Fig. S8 (A) Photocurrent plots of A549 cells at different concentrations on PEC cytosensor. (B) Calibration plot of the PEC cytosensor for different A549 concentrations ((a) 10 cells mL^{-1}, (b) 100 cells mL^{-1}, (c) 1000 cells mL^{-1}, (d) 10000 cells mL^{-1}, (e) 50000 cells mL^{-1}, (f) 100000 cells mL^{-1}).

Reference

1. L. K, Putri, B.-J. Ng, W.-J. Ong, H. W. Lee, W. S. Chang and S.-P. Chai, *ACS Appl. Mater. Interfaces*, 2017, **9**, 4558-4569.